Single Crystal Growths and Characterization of Mercury Based High Temperature Superconductor (Hg-1201)

[1]Than Naing, [2]Xudong Zhao, [3] Xiaoyang Liu

[1]Assistant Lecturer, Department of Chemistry, Dagon University, Myanmar;
[2]Professor, Department of Chemistry, Jilin University, China
[3]Professor, Department of Chemistry, Jilin University, China

Abstract. The mechanism of high-temperature superconductivity still remain mystery and many scientists try to understand it, but there are too many theories and no one is accepted by all people. The uncertainty of experiments is responsible for the difficulty to explain the mechanism of high temperature superconductivity. The compounds $HgBa_2Ca_{n-1}Cu_nO_{2n+2+\delta}$ (Hg12(n-1) n) can be viewed as model systems not only because of their record high-T_c values, but also because of their simplest and high-symmetry crystal structures (P4/mmm). Here we report a novel recipe for the growth of Hg1201 crystals. We improve the previous solid state synthesis, and adopt two-step process for the crystal growth of Hg1201. The magnetic property of Hg1201 crystals were measured with Quantum Design MPMS (SQUID).XPS measurements was used to understand the electronic structure of the cuprates with the concentration of doping.

Keywords: High temperature superconductivity, single crystal growths, SQUID, Raman spectroscopy, XPS

INTRODUCTION

The discovery of superconductivity above the boiling point of liquid nitrogen led to extensive search for new superconducting materials, since the discovery of high transition temperature superconductivity in $La_{2-x}Ba_xCuO_4$ in 1986[1]. Apart from their unusually high values of T_c, these materials also exhibit a variety of complex phenomena and phase. It is well known that Hg-based superconducting cuprates show the highest transition temperature into the superconducting state both at normal pressure and high pressure. That is why these compounds are promising candidates for a number of possible applications.

Putillin et al [2] found that the $HgBa_2CuO_x$ (Hg-1201) compound in 1992, which has only one layer of CuO_2 layer showed a T_c of up to 94K. It was, therefore, rather natural to speculate that T_c can increase if more CuO_2 layers are added in the per unit formula to the compound. Unfortunately, there has been remarkably little scientific work on the mercury based compounds because the availability of sizeable crystals is difficult. Quantitative measurements of any kind would be invaluable benchmarks for testing the theories of high T_c superconductivity.

MATERIALS and METHODS

One of the major difficulties in growing Hg1201 crystals stems is the high vapor pressure of mercury oxide during the crystal growth, which requires encapsulation or high-pressure techniques. In addition, sample preparation must be handled with special care because mercury is highly toxic. Conventional encapsulation is a versatile low-cost setup without constraint in chamber size, but the attainable pressure is constrained by the limited stability of the container. Because Hg easily forms alloys with many metals, typical encapsulation uses quartz, which can contain pressures on the order of 10 bar and is a viable option for Hg1201 synthesis at relative low temperature. A number of groups have obtained small single crystals by this method [2-10]. Based on this method, several improvements have been developed, including the use of a three-zone furnace to control the mercury partial pressure, but yielded crystals less than $1mm^3$ in volume [9,11-14]. To produce large Hg1201 single crystals, we adopted the conventional encapsulation approach, using ordinary box furnaces. The problems usually associated with the high vapor pressure of mercury oxide were solved through two major improvements. First, we found a method to seal thick quartz tubes by welding thick quartz plugs to both ends of the tube, which allowed us to increase the maximum attainable pressure. The sealed tubes are able to withstand a pressure of ≈ 20 bar. Second, we optimized the crystal growth temperature profile to fine-tune the kinetics of the

chemical reaction, in order to reduce the maximum pressure during the growth.

Another major difficulty with the Hg1201 crystal growth is associated with the Ba-Cu-O precursor preparation. Barium oxide is sensitive to carbon contamination (primarily CO_2) and easily forms stable $BaCO_3$, which not only affects the quality of the Hg1201 crystals (as evidenced by a strongly reduced T_c), but also prevents the formation of large single crystals by increasing nucleation centers. As the synthesis of high-quality precursor material with relatively low impurity content to be a very important initial step in the crystal growth, and paid attention to produce a clean precursor containing barium, copper, and oxygen, with the correct stoichiometry of 2:1:3.

Therefore, we adopted a two-step method, first allowing the Ba starting compound $Ba(NO_3)_2$ to partially react with CuO to form a more stable and less carbon-sensitive precursor material.

We designed a special precursor preparation system that employed a quartz kettle and continuous oxygen flow in order to avoid the gas back-flow commonly found in conventional tube furnaces. The stoichiometric ratio of the starting material of $Ba(NO_3)_2$ (99%, Alpha)and CuO (99%, Alpha) were weighed , mixed and well grounded in an agate mortar using some of acetone in order to get a good homogeneity and prevent from the carbon dioxide and water vapor in the atmosphere. After mixing and grinding the powder sample were put in an alumina crucible and which was placed in a home-made kettle that is continually flooded with high-purity oxygen gas.

The $Ba(NO_3)_2$ decomposes thoroughly into NO_2 and BaO at moderate temperature (~ 600 °C), and the emitted NO_2 is then taken away by the oxygen flow and is vented from the kettle and absorbed by a NaOH solution. The freshly generated BaO is rather reactive with CuO, leading to the formation of Ba_2CuO_3. After the mixture of the starting materials is kept at 870 °C for 9 hours, all that remains is the desired precursor material which is a multiphase mixture rather than a single phase compound, and sensitive to CO_2 in air due to existence of barium oxide. We took out the crucible from the furnace when the temperature of the furnace is around 200°C and immediately placed in vacuum desiccators and stored it in a glove-box which fills with an inert gas.

In the second step, 2.14 g of the precursor with the nominal starting composition "$Ba_2Ca_{n-1}Cu_nO_x$" was mixed with 1.50 g of HgO powder and well grounded in a glove-box. The mixture needs to be further contained in a fully-stabilized Zirconia crucible with typical dimensions of 10 mm (inner diameter) and 80 mm (height), in order to prevent CuO from reacting with quartz at elevated temperature. For 2.14 g of the precursor, the stoichiometric amount of HgO (for the creation of Hg1201) is 1.20 g, and the additional 0.30 g of HgO was added in order to compensate for the vaporized Hg and to provide high vapor pressure. By fine-tuning the amount of excess HgO, we were able to optimize growth conditions and avoid the explosion of the sealed quartz tube. In order to hold the pressure, the tubes need to be of reasonable thickness which gives an encapsulation volume that corresponds to a maximal pressure (Hg plus O_2) of ~20 bars during the growth. The Zirconia crucible contained the mixed powder was placed in the quartz tube that is already closed on one end, and sealed it under air evacuated. The sealed quartz tube was placed in a conventional box furnace and heated as shown in the following temperature profile for the synthesis of crystal growth procedure.

The size of the grown crystals varies depending on several factors; some of these factors are difficult to adjust, such as the temperature gradient inside the furnace during the slow-cooling process and the quality of the commercial starting materials from a particular purchase batch. Besides these, a very important factor to grow large single crystal is the amount of contamination from air of the precursor material.

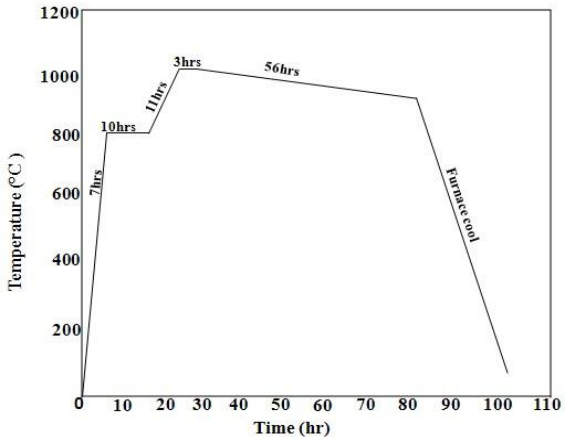

FIGURE 1. Furnace temperature profile for the crystal growth of the Hg1201.

SAMPLE CHARACTERIZATION

X-ray diffraction (XRD) characterization of smaller samples demonstrated that the crystals were typically single phase with the space group of P4/*mmm* and the extracted room-temperature lattice parameters for as -grown crystals were *a* ,*b*= 3.891 Å and *c* = 9.587 Å, and α, β, γ = 90° in

agreement with previously published results [11, 12, 14]. The result of FC/ZFC measurement of an as growth sample of our Hg1201 single crystal is shown in Figure 3. With the field applied along the c-axis, the diamagnetic signal remains almost the same, no matter whether the sample was FC or ZFC. The extremely high ratio between FC and ZFC demonstrates that the sample is of high quality.

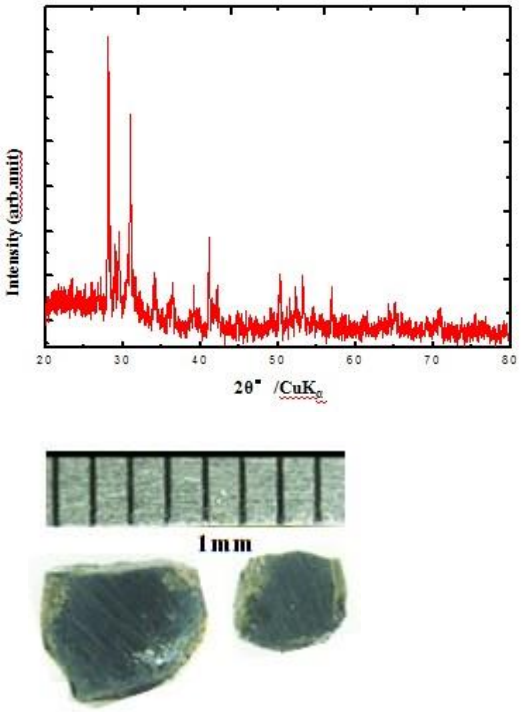

FIGURE 2. Powder X-ray Diffraction patterns of the precursor sample of Hg-1201 and single crystal of Hg-1201.

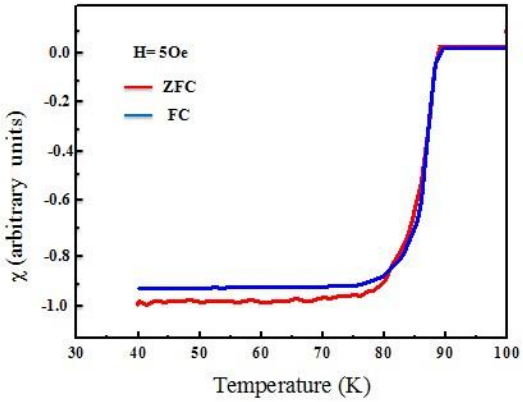

FIGURE 3. Magnetic susceptibility measurements of one of Hg-1201 as-grown sample.

Raman spectroscopy measurement for one of the single crystal of Hg-1201 which has a T_c of 95 K. Raman spectra were obtained by a micro-optical system; excitation was with a 785nm argon-ion laser line. All the spectra were obtained at room temperature. The laser beam was focused on a fixed spot on a crystalline and spectrometer was set at a fixed position to measure the small shift of the Raman bands.

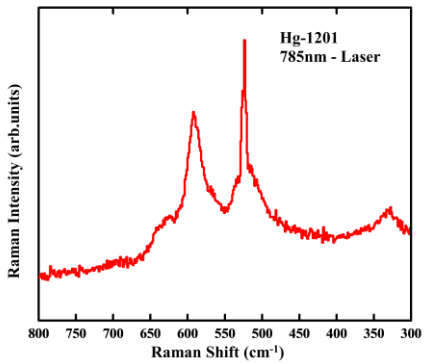

FIGURE 4. Raman spectra of as-grown sample

The two Raman bands at near 591cm^{-1}and 530 cm^{-1} sharp and totally separated. The band at 591cm^{-1} seem reasonable to assign the mode of A_{1g} vibration of the apical oxygen. It is consistent with the results of the previous works by several groups. For the near 530nm peak, Krantz et al.[15] simply attributed to some unidentified defect while Yang et al. presumed it may be Eg mode of the oxygen in the CuO_2 plane. The weak feature near 330cm^{-1} can be attributed to HgO impurity phase.

XPS MEASUREMENT

The XPS spectra were taken using a Surface Science Instrument S-PROBE instrument, using the aluminum K_α line as the X-ray source. The X-rays were reflected onto the sample by a bent-crystal monochromator, with two typically-used spot sizes of 250×1000 or 150×800 μ m^2. The intensity of the X-ray hitting the sample was about 10^{11} photons/cm^2 sec, and the instrumental energy resolution (FWHM) was ~ 1.5 eV in survey scans (wide energy range) and ~1.0 eV in high resolution scans (narrow energy range). The energy resolution is the minimal width of a measured feature, not the uncertainty in the energy reading, which is less than 0.05 eV in high-resolution measurements. Binding energy shifts can be measured with an accuracy of ±40 meV in this fashion [16].

In the XPS measurements, the chemical potential shift is most commonly deduced from the shift of core-level binding energies. In the case of conducting samples, when holes are doped into a system, the chemical potential decreases and

becomes closer to the core levels, which leads to a decrease in the binding energies of the latter. The binding energy shift can be expressed as;

$$\Delta E = \Delta\mu + \Delta V_M + K\Delta Q + \Delta E_R$$

Where $\Delta\mu$, ΔV_M,K, ΔQ ,and ΔE_R represent the change in chemical potential, the change in the Madelung potential, a constant, the change in the valence, and the change in the relaxation energy, respectively[17]. In the cuprates, for core levels of atoms which do not change their valence value upon doping, the terms other than $\Delta\mu$ are usually small, which enables the chemical potential shift to be directly determined by the core level shifts. For core levels of atoms which do change their valence with doping, the fourth term in above equation gives an additional binding energy shift.

Our study of XPS aimed to accurately measure the relative shift of Hg, and to understand the line-shape change of Cu. All of these were obtained as functions of hole (or oxygen) doping.Figure (5) displays wide-range survey scans for five annealing samples (the two UD, the one OPT and the two OV). The spectra of the different samples are highly consistent with each other, both in the peak positions and in the relative intensities of the peaks.

Measurements of the Hg(4f) core level are displayed in Figure(6). As the doping increases, it is observed that the Hg (4f) core levels move further away from the Ba(3d) core levels, since the latter move to lower energies,.This is opposite to the situation regarding Y(3d) and Ba(3d) in YBCO and the reason is not obvious.

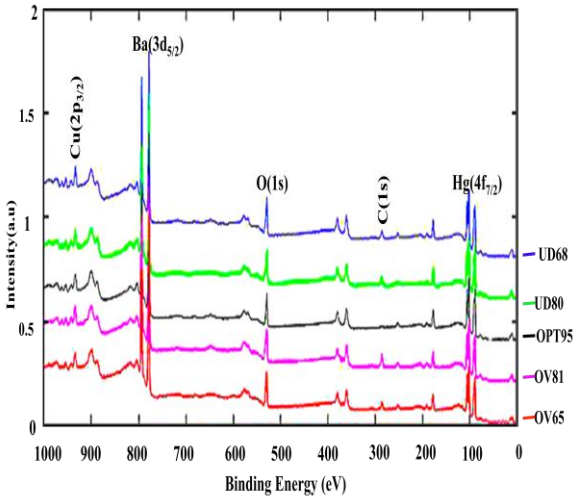

FIGURE 5. Wide-range survey scans for five single crystals of Hg-1201

Barium is highly ionic and always in the Ba^{2+} state in oxides. By adding more oxygen into YBCO and Hg1201, one could imagine that Hg and Y might become more oxidized, and it is known that both the Y(3d) line and the Hg(4f) line move to higher energies in pure oxides when compared to their metallic states [18]. This would

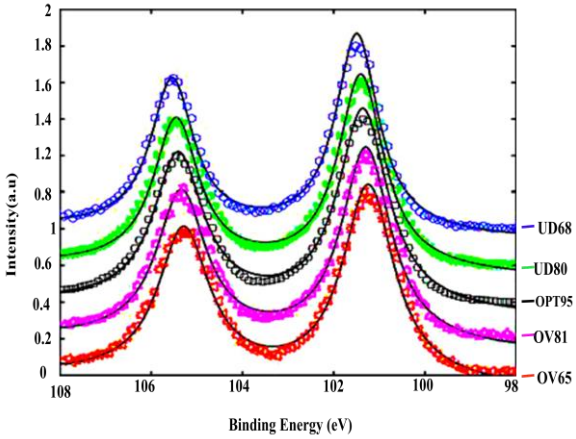

FIGURE 6. Chemical shifts of Hg.

imply that Y(3d) and Hg(4f) both move closer to Ba(3d) with increasing doping, if the relative shifts are purely caused by a valence change of Y and Hg. While this is consistent with the observation for YBCO,[19] the situation for Hg1201 is just the opposite.

A possible explanation was given in [reference 19] for YBCO: the oxygen dopant site O(1) (in the Cu-O chain layer) is rather close to Ba, which might cause additional shifts of the Ba(3d) line through the Madelung potential in above equation and bring the Ba(3d) and Y(3d) lines closer to each other as the doping increases. At first glance, a similar explanation is consistent with our observations for Hg1201, since the oxygen dopant site in Hg1201 is closer to the Hg site than to the Ba site, and one might thus expect an opposite effect from that in YBCO.

While the exact reason for the results of chemical shifts of Hg is not clear, it is possible that there are contributions from the two terms in above Equation. Since a change in the relaxation energy (ΔE_R) has never been observed for the cuprates, there might be a valence change on Hg. Regardless of the underlying reason, the rather linear behavior in Figure(7) suggests that the relative shift between Hg(4f) and Ba(3d) can be used for measuring the oxygen doping level in Hg1201.

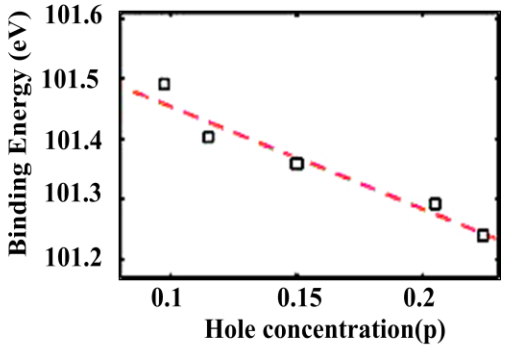

FIGURE 7. The Hg ($4f_{3/2}$) peak center energy as a function of doping. The empirical formula $T_c = T_{c,max}[1 - 82.6(p - 0.16)^2]$ has been suggested to be universal for the hole-doped cuprates.

This may be particularly useful when T_c is no longer as a good indicator of doping, as there are good reasons to believe that the relative shift is solely determined by the amount of dopant oxygen in the Hg plane far from the CuO_2 layer. The method also has the advantage that both the Hg (4f) and Ba(3d) lines are relatively easy to measure with XPS.

Measurements of the Cu ($2p_{3/2}$) peaks are displayed in Figure(8.a)The two peaks are similar to those in pure CuO, with the one near 932.5 eV generally denoted as $2p_{3/2}3d^{10}L$ and the one near 942 eV as $2p_{3/2}3d^9$. The comparison between pure CuO and pure Cu implies that the width of the $2p_{3/2}3d^{10}L$ peak and the relative amplitude between the $2p_{3/2}3d^9$ and $2p_{3/2}3d^{10}L$ peaks can be used as indicators of the valence and the chemical environment of Cu in solids. Indeed, the most prominent changes in the Cu spectrum of Hg1201 with doping are the development of a high-energy shoulder on the $2p_{3/2}3d^{10}L$ peak (indicated by arrow 3 in Figure (8(a)) and the increasing amplitude of the $2p_{3/2}3d^9$ peak (arrow 2), both of which are consistent with the expectation that holes are doped into the CuO_2 layers.

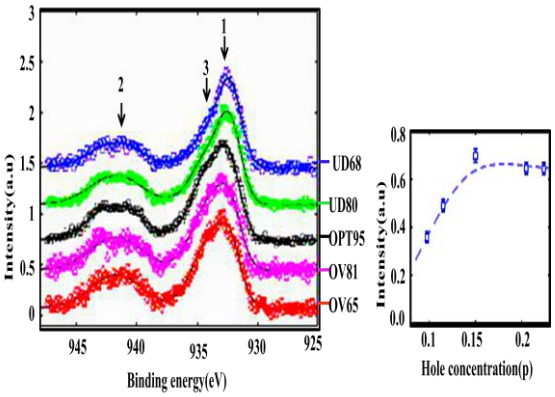

(a) (b)

FIGURE 8. (a) Line-shape changes of Cu. The data have been calibrated using the Ba(3d) line and several measurements for each doping have been averaged. Solid lines are fits to the data. **(b)** Intensity of the shoulder (arrow 2) in figure (a) as a function of doping.

The common belief is that when holes are doped into the CuO_2 layer, they mainly go to the O sites, because the second electron affinity energy of O is much lower than the third ionization energy of Cu. In other words, as more O is added into the Hg-O layer, the valence of Cu barely changes, but the O in the CuO_2 layer possesses a less negative valence.

When an electron is knocked out by a photon and a core hole is created in the Cu (2p) orbital, the final energy of the photoelectron (measured by XPS) depends on how the core hole is screened by its surroundings. The photoelectron contributes to the intensity in the locally screened channel when the core hole only attracts electrons that are very nearby, mostly from other orbitals of the same Cu atom, which results in relatively poor screening of the core hole and causes it to attract the photoelectron more on the latter's way out, leading to a higher binding energy. Nonlocal screening takes place when the core hole is also allowed to attract electrons from neighboring oxygen orbitals, which results in better screening and a lower binding energy for the photoelectron. In this regard, when a lot of holes are already doped into the CuO_2 layers, which mostly deplete electrons in the oxygen orbitals (through the formation of the so-called Zhang-Rice singlets surrounding Cu), a core hole has a lesser chance of being nonlocally screened, and therefore the spectral weight shifts into the shoulder in Figure (8a).

The shoulder (peak 3 in Figure.8a) is generally referred to as the locally screened channel, whereas the main peak (peak 1 in Figure.8a) is referred to as the nonlocal screening channel [20-24]. In order to quantify the key observations, the

amplitudes of peak 3 are plotted as a function of doping in Figure 8(b), the high-energy shoulder of the $2p_{3/2}3d^{10}L$ feature undergoes a clear saturation near optimal doping. There are two intuitive candidate explanations for this shoulder. The first explanation is that adding oxygen into the Hg layer changes the Cu valence in the CuO_2 layer. The second explanation is that the Cu ions experience a change in the local chemical environment with oxygen doping. Given that the $2p_{3/2}3d^9$ features is absent in pure Cu but is present in pure CuO, its independence of doping strongly suggests that the valence of copper remains constant, and that it is the chemical environment of Cu that changes with doping.

The saturation in figure 8(a) near optimal doping seems to imply that "overdoping" might have nothing to do with the CuO_2 layers, at least not in the sense of altering the screening behavior for the Cu core holes. Since the CuO_2 layer is never truly heavily doped, i.e., there are always plenty of electrons in the O (2p) orbital, the most natural explanation is that additional holes beyond optimal doping do not go into the O(2p) orbital at all. On the other hand, from the relative shift between Hg(4f) and Ba(3d), it seems that the dopant oxygen in the Hg-O layer are playing a similar role on both sides of the superconducting dome (except for creating a subtle broadening of the Hg(4f) peak which also saturates around optimal doping). In other words, some holes are still being doped into the system on the overdoped side, and the most likely alternative orbital that these holes can go to are the apical oxygen orbitals. While the exact interpretation of our XPS results warrants further investigation, it is quite clear that hole-doping involves more than simply the CuO_2 layers, and it might not involve the CuO_2 layers at all on the overdoped side. The pseudogap phase might terminate just slightly above optimal doping, and is related to magnetic degrees of freedom that involve the apical oxygens. It remains an intriguing open question whether the holes that presumably end up in the apical oxygen orbitals are the cause for the pseudogap to disappear.

CONCLUSION

The model compound Hg-1201 which exhibits the highest superconducting transition temperature of all single-layer cuprates. The size of the grown crystals varies depending on several factors. For unknown reasons, it has been found that, in order to grow large single crystals, a small amount of air contamination is needed. According to XPS measurement, some holes are still being doped into the system on the overdoped side; these holes can go to the apical oxygen orbital.

ACKNOWLEDGEMENT

First of all, I would like to acknowledge my research supervisors, Prof. Xudong Zhao and Prof. Xiaoyang Liu (Jilin University, Changchun, China) for giving me the opportunity to work under their command and also for all the support, guidance and encouragement throughout these years. I am also deeply grateful to Pro-rector Dr. Aye Aye Tun (Dagon University, Myanmar) and Prof. Dr. Cho Cho Win (professor, Chemistry department, Dagon University, Myanmar) for giving me the opportunity to participate seventh global conference on Power Control and Optimization (PCO 2013). I appreciate the significant assistance of all my colleagues from Jilin University in China, especially.

REFERENCES

1. J. G. Bednorz, K. Müller, *Z. Phys. B* **1986**, *64*,189.
2. SN Putillin, EV Antipov, O Chmaissem, M Marezio. Superconductivity at 94 K in $HgBa_2CuO_{4+\delta}$. Nature 362:226–228, 1993.
3. A. Yamamoto, K. Minami, W. Z. Hu, A. Miyakita, M. Izumi, and S. Tajima. Effects of Zn substitution on the superconductivity and pseudogap in $HgBa_2CuO_{4+\delta}$ with various doping levels. *Phys. Rev. B*, 65:104505, 2002.
4. A. Schilling, M. Cantoni, J. D. Guo, and H. R. Ott. Superconductivity above 130 K in the Hg-Ba-Ca-Cu-O system. *Nature*, 363:56, 1993.
5. D. Pelloquin, V. Hardy, A. Maignan, and B. Raveau. Single crystals of the 96K super conductor $(Hg,Cu)Ba_2CuO_{4+\delta}$: growth, structure and magnetism. *Physica C*, 273:205, 1997.
6. A. J. Batista-Leyva, M. T. D. Orlando, L. Rivero, R. Cobas, and E. Altshuler. The resistive transition of $(Hg_{0.85}Re_{0.15})$ $(Ba_{2-y}Sr_y)$ $Ca_2Cu_3O_{8+\delta}$ superconducting polycrystals. *Physica C*, 383:365, 2003.
7. C.T.Lin, Y.Yan, K.Peters, E.Schonherr, and M. Cardona. Flux growth of $Hg_{1-x}Re_xBa_2Ca_{n-1}Cu_nO_{2n+2+\delta}$ single crystals by self-atmosphere. *Physica C*,300:141, 1998.
8. A.Kareiva and I.Bryntse. A novel synthesis route to the mercury-containing superconductor $HgBa_2CaCu_2O_{6+\delta}$ partly based on the sol-gel technique. *J.Mater. Chem.*, 5:885, 1995.
9. K. Knizek, M. Veverka, E. Hadova, J. Hejtmanek, D. Sedmidubsky, and E. Pollert. Synthesis of $HgBa_2CuO_{4+\delta}$ by sol-gel method under controlled oxygen pressure, electron, and thermal transport properties. *Physica C*, 302:290,1998.
10. Meng R L, Beauvais L, Zhang XN, et al. Synthesis of the high-temperature superconduct -ors $HgBa_2CaCu_2O_{6+\delta}$ and $HgBa_2Ca_2Cu_3O_{8+\delta}$

[J]. Physica C-Superconductivity and Its Applications, 1993, 216: 21.

11. Y. Zhao, B. Chen, M. Larobina, H. L. Kennedy, and P. Fekitoa. Superconductivity at 134 K in $HgBa_2Ca_2Cu_3O_y$ prepared using a dual hot-zone furnace. *J.Mater. Sci. Lett.*, 15:323, 1996.
12. V. A. Alyoshin, D. A. Mikhailova, and E. V. Antipov. Synthesis of $HgBa_2CuO_{4+\delta}$ under controlled mercury and oxygen pressures. *Physica C*,271:197, 1996.
13. S. Lee, M. Mun, M. Bae, and S. Lee. Synthesis and superconducting properties of $HgBa_2Ca_2Cu_3O_{8+\delta}$. *J. Mater. Chem.*, 4:991, 1994.
14. G. B. Peacock, I. Gameson, and P. R. Edwards. Bulk synthesis of the 135 K superconductor $HgBa_2Ca_2Cu_3O_{8+\delta}$. *Adv. Mater.*, 9:248, 1997.
15. Krantz , M.C. , Thomsen , C. , Mattausch , H.J. , and Cardona , M. (1994) Phys. Rev. B , 50 , 1165 – 1170 .
16. A. Ino, T. Mizokawa, A. Fujimori, K. Tamasaku, H. Eisaki, S. Uchida,T. Kimura, T. Sasagawa, and K. Kishio. Chemical potential shift in overdoped and underdoped $La_{2-x}Sr_xCuO_4$. Phys. Rev. Lett., 79:2101{2104, 1997.
17. B. V. Crist. Handbook of monochromatic XPS spectra. XPS International, LLC, 1999.
18. S. H□ufner. Photoelectron Spectroscopy, chapter 2, page 35. Springer-Verlag, 1995.
19. K. Maiti, J. Fink, S. de Jong, M. Gorgoi, C. Lin, M. Raichle, V. Hinkov, M. Lambacher, A. Erb, and M. S. Golden. Doping dependence of the chemical potential and surface electronic structure in $YBa_2Cu_3O_{6+x}$ and $La_{2-x}Sr_xCuO_4$ using hard X-ray photoemission spectroscopy. Phys. Rev. B, 80:165132, 2009.
20. M. A. van Veenendaal, H. Eskes, and G. A. Sawatzky. Strong nonlocal contributions to Cu 2p photoelectron spectroscopy. Phys. Rev. B, 47:11462{11469,1993.
21. M. A. van Veenendaal and G. A. Sawatzky. Nonlocal screening effects in 2p X-ray photoemission spectroscopy core-level line shapes of transition metal compounds.Phys. Rev. Lett., 70:2459{2462, 1993.
22. K. Karlsson, O. Gunnarsson, and O. Jepsen. Cuprate core-level line shapes for different Cu-O networks. Phys. Rev. Lett., 82:3528{3531, 1999.
23. A. Koitzsch, J. Fink, M. S. Golden, K. Karlsson, O. Jepsen, O. Gunnarsson, L. L. Miller, H. Eisaki, S. Uchida, G. Yang, and S. Abell. Core-hole screening response in two-dimensional cuprates: A high resolution X-ray photoemission study. Phys. Rev. B, 66:024519, 2002.